Granular Matter (2019) 21:13
https://doi.org/10.1007/s10035-019-0865-y

ORIGINAL PAPER

Discrete element modeling of first shear strain gradient effects on mechanical behaviors in granular materials

Shu-Mei Yang[1] · **Wen-Ping Wu**[1,2] · **Ming-Xiang Chen**[1,2]

Received: 12 April 2018 / Published online: 21 January 2019

Abstract

The effects of strain gradient on the mechanical behavior of granular materials have attracted attention from many researchers. In this paper, the effects of the first shear strain gradient in granular materials are focused on. Granular assemblies with various particle radii and porosities are built through a two-dimensional discrete element method (2D-DEM) simulations. The results indicate that the macro shear stress is insensitive to the first shear strain gradient at low strains, but is indeed affected at high strains; the third order stress conjugated with the first shear strain gradient is sensitive to the first shear strain gradient in all deformation cases; the third order work done by the third order stress and the ratio of it versus the total work are affected by the first shear strain gradient; the evolutions of the invariants of the third order stresses present severe change of the local relative vertical displacement of particles, which lead to localization occurrence. Based on DEM simulations, it is found that only the effect consideration of the first shear strain gradient on the macro shear stress is not sufficient, whereas the effect on work should also be taken into account and the third order work as a part of strain energy cannot be ignored, which is falsely classified as a portion of the accumulated energy dissipated by frictional sliding.

Keywords First shear strain gradient · Macro shear stress · Third order stress · Third order work · Granular materials

List of symbols

$A(t)$	Shape parameter of the primary term of displacement
$B(t)$	Shape parameter of the quadratic term of displacement
c	Ratio of $B(t)$ versus $A(t)$
$\overline{\sigma}_{12}$	Macro shear stress
$\overline{\Sigma}_{221}$	Third order stress which is conjugated with the first shear strain gradient
W_1	Second order work, the integral of the macro shear stress times the macro shear strain in total volume
W_2	Third order work, the integral of the third order stress times the first shear strain gradient in total volume
W	Summation of W_1 and W_2
α	Ratio of W_2 versus W
F_1, F_2, F_3, F_4, F_5	Five invariants of the conjugated stresses

1 Introduction

Due to the corresponding discontinuous nature, the mechanical behaviors of granular materials are significantly complex; therefore the experiments are quite difficult to be conducted. To describe the mechanical behaviors of granular materials [1–3], many effective methods have been developed such as the Distinct Element Method (DEM) proposed by Strack and Cundall [4]. Also, to simplify the granular material constitutive relation, the granular material was regarded as a simple material in many researches. The concept of *simple material* was defined by Noll [5, 6], where the stress at one point of this material had a simple connection with the strain and the corresponding history at that point. This simple relation

✉ Wen-Ping Wu
wpwu@whu.edu.cn

✉ Ming-Xiang Chen
mxchen@whu.edu.cn

[1] Department of Engineering Mechanics, School of Civil Engineering, Wuhan University, Wuhan 430072, China

[2] State Key Laboratory of Water Resources and Hydropower Engineering Science, Wuhan University, Wuhan 430072, China

constituted this material different from other materials. Based on the Noll concept, Kuhn [7, 8] verified that a granular material was not a simple material, whereas the stress at one point not only depended on the strain and the corresponding history, but also the strain gradients, where a relationship with the high order quantity of deformation gradient had been established.

The strain gradient effects were first proposed by Mindlin [9], where the potential energy–density was considered as a function of strain as well as its first and second gradients. Consequently, a quite generalized simplification theory that contained only the strain and the corresponding first derivative was put forward. Subsequently, many researchers, such as Fleck et al. [10, 11], Yang et al. [12] and Gao et al. [13] improved and enriched this theory, afterwards, Yang and Misra [14] presented a second gradient stress–strain damage elasticity theory to simulate shear bond localization based upon the method of virtual power, and then Placidi et al. [15] provided analytical solutions of identifying all the constitutive parameters of the 2D solids characterized by a strain energy dependent on the first and second gradient of the displacement. For granular materials, the strain gradient effects had been postulated and many gradient-dependent constitutive formulations had already been proposed, where the granular material was considered as a continuum at the macro scale, indifferently to the constitutive formulation. Chang and Gao [16] reported the displacement and rotation fields by continuous polynomial functions and various classes of continua, including the High-gradient continua and the First-gradient continua. In order to describe the evolutions of mechanical quantities realistically in granular materials, Chang and Kuhn [17] further utilized the virtual work concept to obtain expressions of conjugate forces, which were conjugated with various strain gradients. Consequently, the effects of strain gradient on the strain localization were investigated [18]. Voyiadjis et al. [19] proposed a constant internal length scale to describe the shear band thickness. Hattamleh et al. [20] discovered that the gradient term diffused the concentration of plastic strains within shear band. Following, Kuhn [8] verified the softening effect of the first shear strain gradient and the hardening effect of the second shear strain gradient on the macro stress under high strain. Subsequently, the strain gradient effects on the localizations of granular materials were studied [21], which were mainly focused on the relationship of macro stress and strain. Recently, Misra and Poorsolhjouy [22, 23] obtained higher-order elastic constants for grain assemblies by introducing higher gradients, and presented a method to identify the macro and microscale constitutive coefficients from discrete simulation which consider the first and second displacement gradients. By contrast with the research of macro stress and strain, the effects of various strain gradients on the work were not deeply discussed, where the higher order term contribution to the energy was ignored, which might have led to a non-conservation of energy.

In this paper, the effects of first shear strain gradient on the mechanical behaviors of granular materials are investigated. Non-uniform displacement patterns are applied to granular assemblies and the displacement fields are assumed as continuous polynomial functions. The variations of macro shear stress and the conjugated stress under various strain gradient loads are mainly focused on, subsequently the porosity and particle radius of the granular assemblies are changed to study the effects of various gradients on mechanical behaviors. Through the analysis of macro shear stress and conjugated stress, as well as the work and invariants versus the macro shear strain, the effects of the first shear strain gradient on mechanical behaviors of granular materials can be demonstrated, possibly constituting a qualitative analysis method for granular materials.

2 Homogenization

2.1 From discrete particles to continuum field

Granular materials are known as a collection of particles with various sizes and shapes, where voids exist among particles. Consequently, the granular materials are a discontinuum system with particles and voids, which display discrete velocity and displacement, but the stress is a continuum concept. Therefore a connection between the discrete displacement system and the continuous force system must be made.

To develop a continuum mechanics model for the behavior of a particle assembly, it is desirable to view the discrete system as an equivalent continuum system. Therefore, the displacement and rotation of discrete particles are defined as macro-scale continuum fields, which utilize a polynomial expansion [24, 25]. The detailed expressions are as follows:

$$u_i(X) = \overline{u_i} + \overline{u_{ij}} x_j + \frac{1}{2}\overline{u_{ijk}} x_j x_k \tag{1}$$

where u_i represents the displacement and rotation of an arbitrary point in an assembly, $\overline{u_i}$ stands for the rigid displacement of an assembly, respectively. $\overline{u_{ij}}$ and $\overline{u_{ijk}}$ can be utilized to describe the deformation characteristics; $\overline{u_{ij}}$ is the macro strain, $\overline{u_{ijk}}$ is the strain gradient, respectively. The coordinates x_j are measured from the centroids of volume V.

Following, to obtain the expressions of the virtual work, the virtual displacement and rotation must be provided; the expressions are as follows as Eq. (2).

$$\delta\hat{u}_i(X) = \delta u_i^0 + \delta u_{ij}^0 x_j + \frac{1}{2}\delta u_{ijk}^0 x_j x_k \tag{2}$$

The concrete meanings of δu_i^0, δu_{ij}^0, and δu_{ijk}^0 are the same as the $\overline{u_i}$, $\overline{u_{ij}}$ and $\overline{u_{ijk}}$, which can be utilized as the virtual deformation characteristics.

2.2 Principle of virtual work

For a granular material system, a principle of virtual work in a discrete system could be obtained following the approach by Chang et al. [24, 25]. By multiplying the each equilibrium equations of interior and boundary particles, the virtual work can be obtained as follows. The second term of Eq. (3) will always be zero, by introducing the supplementary independent virtual displacement δu_i^b of the boundary contact points themselves, superior stress expressions can be obtained.

$$\delta W^d = \frac{1}{V}\sum_n \left(\sum_{b\in B} f_i^{nb} + \sum_{m\in V} f_i^{nm}\right)\delta u_i^n + \frac{1}{V}\sum_{b\in B}(f_i^b - f_i^b)\delta u_i^b = 0 \tag{3}$$

where f_i^{nb} represents the contact force of a peripheral particle, n and m represent the internal particles, b represents the external contact, f_i^{nm} represents the contact force of inner particles.

Subsequently, the virtual work can be divided into two parts. The first part is an external virtual work associated with the boundary displacements and the second part is an internal virtual work associated with the internal deformation. The corresponding expressions are as follows:

$$\delta W^d = \delta W_E^d - \delta W_I^d = 0 \tag{4}$$

$$\delta W_E^d = \frac{1}{V}\sum_{b\in B} f_i^b \delta u_i^b \tag{5}$$

$$\delta W_I^d = -\frac{1}{V}\sum_n \sum_{m\in V} f_i^{nm}\delta u_i^n + \frac{1}{V}\sum_{b\in B} f_i^b(\delta u_i^b - \delta u_i^n) \tag{6}$$

Substituting Eq. (2) into Eqs. (4), (5) and (6), the expressions of the virtual work, including δu_i^0, δu_{ij}^0 and δu_{ijk}^0, can be obtained. Since the interior and exterior virtual works must be equal for an arbitrary selection of the macro strains,the following equivalences among the force sums can be obtained.

$$\begin{aligned}\frac{1}{V}\sum_{b\in B} f_i^b x_j^b &= \frac{1}{V}\sum_{c\in V\cup B} f_i^c l_j^c \\ \frac{1}{V}\sum_{b\in B} f_i^b x_j^b x_k^b &= \frac{1}{V}\sum_{c\in V\cup B} f_i^c J_{jk}^c\end{aligned} \tag{7}$$

where f_i^c is the contact force of particles, l_j^c is the branch vector which connects the reference points X^m and X^n of particles, J_{lj}^c is a quadratic parameter which is related to X^m and X^n.

Based on the virtual macro strain of a representative volume element, the expression of virtual work can be written as follows, where the macro stress is conjugated with the macro strain.

$$\begin{aligned}\delta w &= \bar{\sigma}_{ji}\delta u_{ij}^0 + \bar{\sum}_{kji}\delta u_{ijk}^0 \\ \bar{\sigma}_{ji} &= \frac{1}{V}\sum_{c\in V\cup B} f_i^c l_j^c, l_j^c = x_j^m - x_j^n \\ \bar{\sum}_{kji} &= \frac{1}{2V}\sum_{c\in V\cup B} f_i^c J_{jk}^c, J_{jk}^c = x_i^m x_j^m - x_i^n x_j^n\end{aligned} \tag{8}$$

2.3 Invariants of third order stresses

Based on the symmetry of third order stresses $\overline{\Sigma}_{ijk}=\overline{\Sigma}_{jik}$, five invariants exist [26–32],

$$\begin{aligned}F_1 &= \overline{\Sigma}_{111}^2 + \overline{\Sigma}_{222}^2 + \overline{\Sigma}_{112}^2 + \overline{\Sigma}_{221}^2 + 2\overline{\Sigma}_{112}\overline{\Sigma}_{222} + 2\overline{\Sigma}_{111}\overline{\Sigma}_{221} \\ F_2 &= \overline{\Sigma}_{111}^2 + \overline{\Sigma}_{122}^2 + \overline{\Sigma}_{211}^2 + \overline{\Sigma}_{222}^2 + 2\overline{\Sigma}_{111}\overline{\Sigma}_{122} + 2\overline{\Sigma}_{211}\overline{\Sigma}_{222} \\ F_3 &= \overline{\Sigma}_{111}^2 + \overline{\Sigma}_{122}^2 + \overline{\Sigma}_{211}^2 + \overline{\Sigma}_{222}^2 + 2\left(\overline{\Sigma}_{112}^2 + \overline{\Sigma}_{221}^2\right) \\ F_4 &= \overline{\Sigma}_{111}^2 + \overline{\Sigma}_{222}^2 + \overline{\Sigma}_{112}^2 + \overline{\Sigma}_{221}^2 + 2\overline{\Sigma}_{112}\overline{\Sigma}_{211} + 2\overline{\Sigma}_{122}\overline{\Sigma}_{221} \\ F_5 &= \overline{\Sigma}_{111}\overline{\Sigma}_{211} - \overline{\Sigma}_{111}\overline{\Sigma}_{112} - \overline{\Sigma}_{122}\overline{\Sigma}_{112} - \overline{\Sigma}_{122}\overline{\Sigma}_{222} + \overline{\Sigma}_{211}\overline{\Sigma}_{221} + \overline{\Sigma}_{222}\overline{\Sigma}_{221}\end{aligned} \tag{9}$$

3 Simulation models and methods

3.1 Simulation models

The particle flow code (PFC) numerical simulation as a discrete element method (DEM) is constantly used in the research of basic physical and mechanical properties of granular materials [4, 33–35]. In this paper, the PFC2D is utilized to simulate the strain gradient effects on the mechanical properties of the granular materials. The modeling box of a granular assembly is 0.2×0.2 m, six granular assemblies are built. The particle radius and porosity are two variables in model building, while the other quantities are the same. Two particle radii are utilized. One radius is the radius of all particles of 0.001 m, whereas the other radius is the radius range of 0.0008–0.001 m. Moreover, three porosities are utilized as 0.11, 0.172 and 0.21. Furthermore, the contact model of the particles is linear, the stretch stiffness and shear stiffness are 1e7 N/m, the friction coefficient is 0.5, whereas no rolling resistance is included in the contact mechanism. The parameters are chosen on an empirical basis [33–35], as listed in Table 1. The particles are initially assembled and compacted into an irregular arrangement, but macroscopically isotropic.

Table 1 Parameters of simulations and material properties of granular assemblies

Parameters	Values
Geometrical size	0.2 × 0.2 m
Radii of particles	0.001 m and 0.0008–0.001 m
Initial porosity	0.11, 0.172 and 0.21
Particle density	1400 kg/m^3
Local damping	0.7
Normal spring constant	1e7 N/m
Tangential spring constant	1e7 N/m
Friction coefficient	0.5

3.2 Methods

Different from Kuhn's algorithm [7], the displacement loading instead of the force loading is directly utilized to form a non-uniform displacement field in this paper as showed in Fig. 1, and the common boundary condition instead of the periodic boundary condition is used. The effects of first shear strain gradient on the mechanical behavior of the granular material during the shear testing are discussed.

In the tests of constrained deformation, all particles of an assembly are slowly and progressively generated shear deformation through a sequence of horizontal displaced shapes $U1$ as showed in Fig. 2:

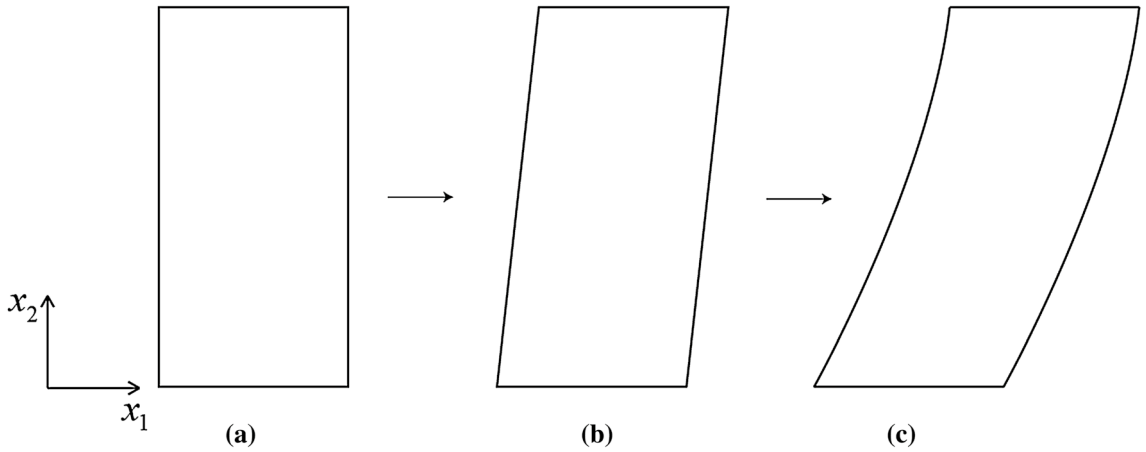

Fig. 1 Deformation diagram of granular material under displacement load application, from (**a**) to (**b**), then to (**c**)

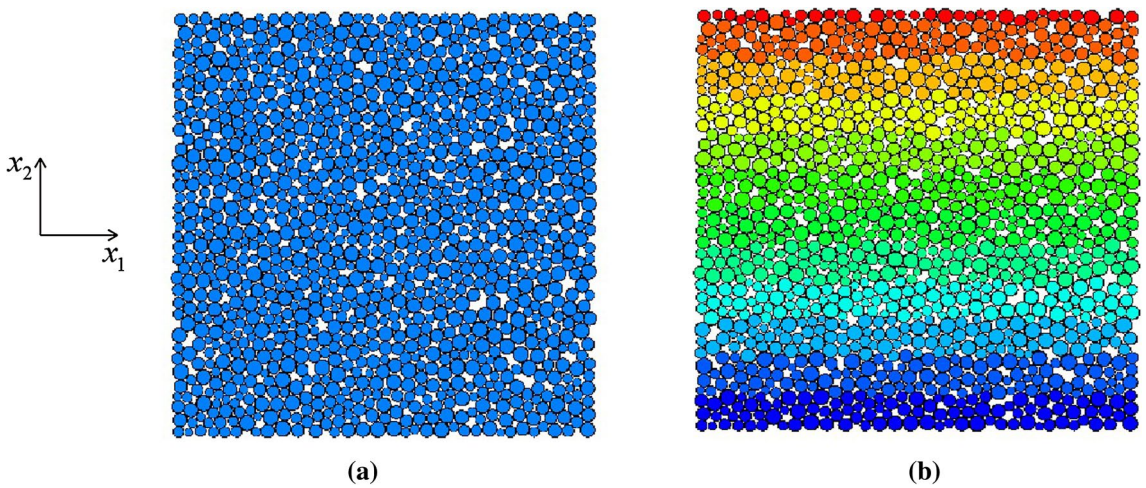

Fig. 2 **a** simulated model in PFC 2D; **b** displacement pattern applied to granular material in PFC 2D

$$U1 = A(t)x_2 + \frac{1}{2}B(t)x_2^2 \tag{10}$$

where$A(t)$ and $B(t)$ are two shape parameters, $U1$ is predetermined through the change of the former. Following, the horizontal shear strain $\varepsilon(x_2, t)$ and the first shear strain gradient $\eta(x_2, t)$ are calculated as follows:

$$\begin{aligned} \varepsilon(x_2, t) &= \frac{\partial U1}{\partial x_2} = A(t) + B(t)x_2 \\ \eta(x_2, t) &= \frac{\partial^2 U1}{\partial x_2^2} = B(t) \end{aligned} \tag{11}$$

In the simulations, the values of $A(t)$ and $B(t)$ are advanced in small steps until the required values are satisfied. The $A(t)$ has a required value, through setting the constant ratio c of $B(t)$ versus $A(t)$, which are set as 0, 1, 3, 5, 7 and 10, then the required value of $B(t)$ can be obtained. Consequently, the mechanical behaviors of various assemblies under various displacement patterns are discussed.

4 Results and discussion

Six granular assemblies are simulated to observe the mechanical behaviors through PFC2D. The evolution processes of the macro shear stress versus the macro shear strain in the simulations are observed. Consequently, the values of the work and the invariants can be calculated through Eqs. (8) and (9). The results are analyzed from three aspects: one aspect is the macro shear stress and the third order stress, the second aspect is the work and the third aspect

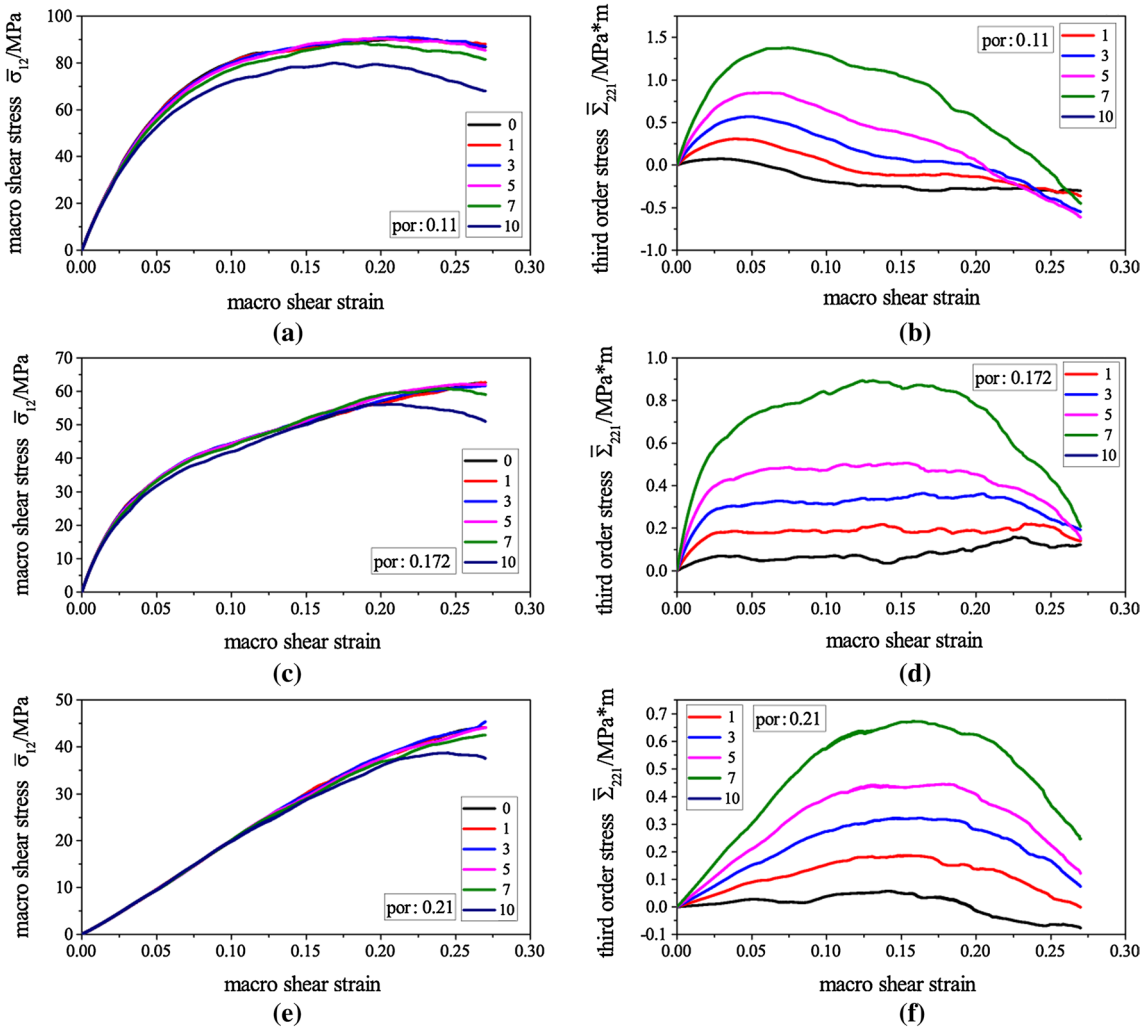

Fig. 3 Macro shear stress and third order stress versus macro shear strain curves under six displacement patterns of ratio c, set as 0, 1, 3, 5, 7, 10 for **a**, **b** assembly of porosity of 0.11; **c**, **d** assembly of porosity of 0.172; **e**, **f** assembly of porosity of 0.21, granular assemblies with the radius of 0.001 m

is the invariants. Following, the effects of first shear strain gradient on the mechanical behavior of the granular material can be presented.

4.1 Evolution of macro shear stress and third order stress

Figures 3 and 4 present the evolutions of the macro shear stress $\overline{\sigma}_{12}$ and the third order stress $\overline{\Sigma}_{221}$ versus the macro shear strain under six displacement patterns of the ratio c, set as 0, 1, 3, 5, 7 and 10. Figure 3 presents the characteristics of granular assemblies with the radius of 0.001 m and Fig. 4 presents the characteristics of the granular assemblies with the radius of 0.0008–0.001 m. No matter what the granular assembly is, the same phenomenon can be observed.

Under low strains, the macro shear stress is insensitive to the first shear strain gradient, but the first shear strain gradient effect on the third order stress is apparent, for which, as the first shear strain gradient increases, the third order stress increases when the same macro shear strain is achieved. These results are in accordance with the predictions of the theory in Ref. [5]. The integral of the first shear strain gradient in total volume is zero under low strains, which means that the shear strain gradient does not contribute to the shear strain, while the values of the shear strain are the same under different displacement patterns. Therefore, the evolution curves of the macro shear strain are insensitive to the first shear strain gradient under low strains.

Under high strains, when the macro strain exceeds a certain value as shown in Figs. 3 and 4, the macro shear stress is sensitive to the shear strain gradient. The third order stress

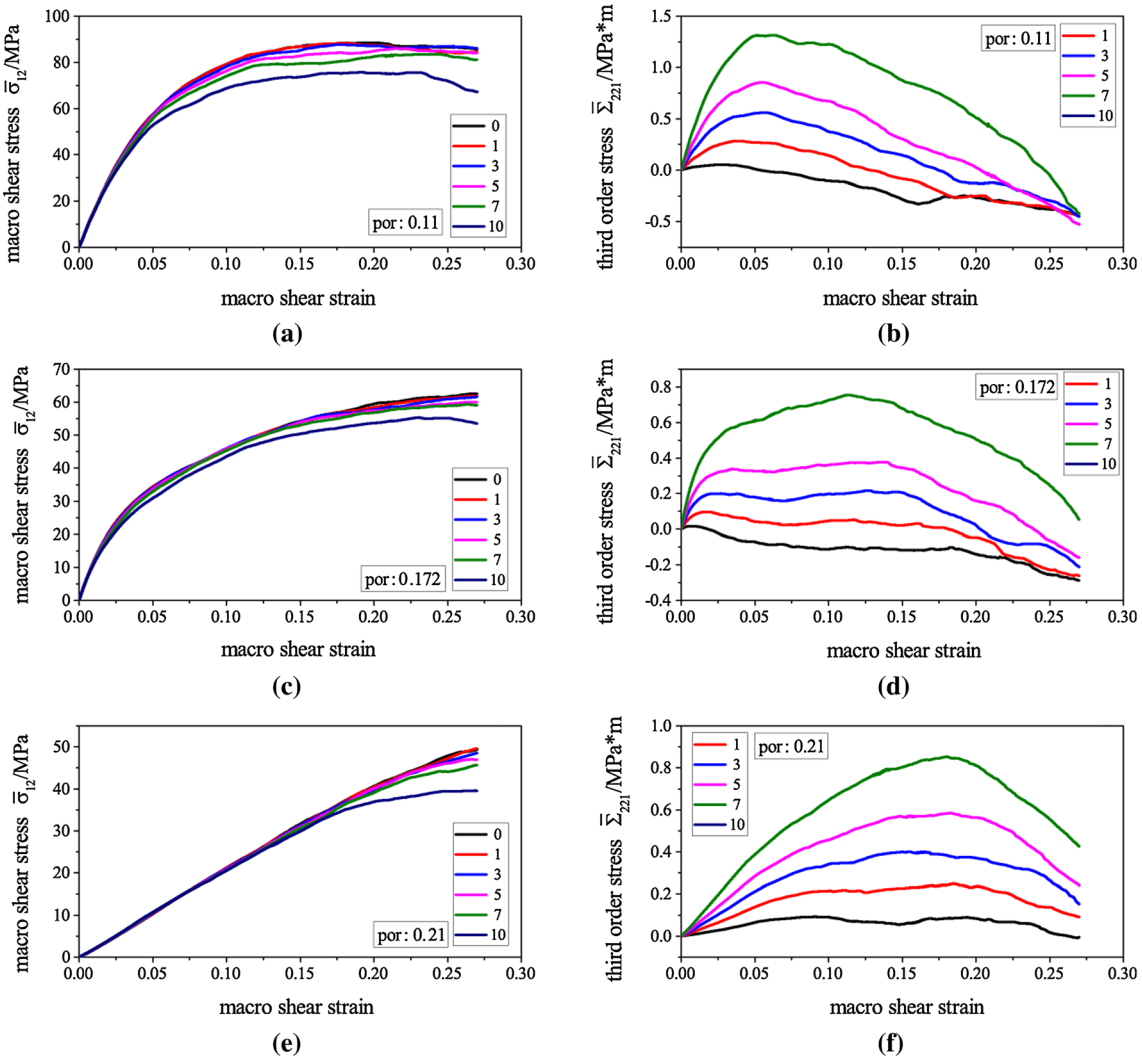

Fig. 4 Macro shear stress and third order stress versus macro shear strain curves under six displacement patterns of ratio c, set as 0, 1, 3, 5, 7, 10 for **a**, **b** assembly of porosity of 0.11; **c**, **d** assembly of porosity of 0.172; **e**, **f** assembly of porosity of 0.21, granular assemblies with the radius of 0.0008–0.001 m

also changes significantly under different displacement patterns. When the deformation gradually increases to exceed the low strains range, the initial configuration no longer overlaps with the current configuration, the integral of the shear strain gradient in total volume is not zero under low strains and the macro shear stress will be different when the same macro shear strain is achieved. This demonstrates that the macro shear stress value is related to the macro shear strain and the first shear strain gradient. The granular material is not a simple material. The representative volume element behaves as a higher order continuum, even though each point within the representative volume element is a classic continuum.

As shown in Fig. 4, as the first shear strain gradient increases, the change of the macro shear stress is increasingly apparent. The stress change ratio $((\overline{\sigma}_{12}^{c=cur} - \overline{\sigma}_{12}^{c=0})/\overline{\sigma}_{12}^{c=0})$, can be observed in Fig. 5. As the first shear strain gradient increases, the stress change ratio is not monotonous, but fluctuant. Adversely, when the first shear strain gradient increases, the effect on the macro shear stress is quite apparent, even reaching −27% (see Fig. 3a), in which minus (−) means that the first shear strain gradient has a softening effect on the macro-stress, when the first shear strain gradient increases to a certain extent.

For granular assemblies with different porosities and particle radii, the trend impact is the same, but the effect extent differs. When assemblies are enforced to the same displacement pattern of the ratio c set as 10, as the porosity increases, the stress ratio for the assembly with the radius of 0.001 m decreases from −27.7 to −22.6%, as well as subsequently to −15%, while the stress ratio for the assembly with the radius of 0.0008–0.001 m decreases first from −21.5 to −14.4%, subsequently increasing to −20%. This is related to the microstructure of assemblies and requires further research.

4.2 Work evolution

The concept of the work is significantly important in mechanics, since it explains the energy in granular materials. A linear contact model defines three energy partitions in the PFC, which are the strain energy, the slip energy and the dashpot energy. The strain energy is defined as the energy stored in the springs, the slip energy is defined as the accumulated energy dissipated by frictional sliding, whereas the dashpot energy is defined as the accumulated energy dissipated by the viscous dashpots. In this paper, a linear contact model is used, where only two energy partitions exist because the dashpot quantity is set to zero.

Chang et al. [15] obtained the expression of virtual work in granular materials; consequently the expression of work could be obtained when the virtual displacement is the actual displacement. If the quadratic term of displacement could not be ignored, the first shear strain gradient will exist. The expression of the work is made up of two parts, which are the second order work and the third order work. The second

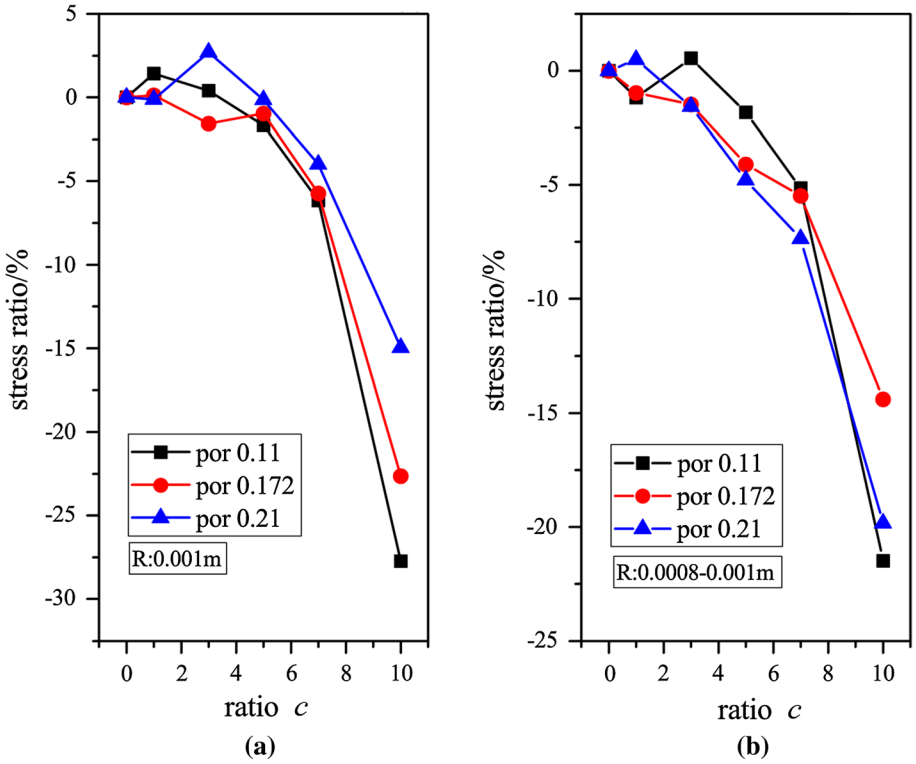

Fig. 5 The stress ratio versus ratio c curves under six displacement patterns for **a** assembly with the radius of 0.001 m; **b** assembly with radii of 0.0008–0.001 m

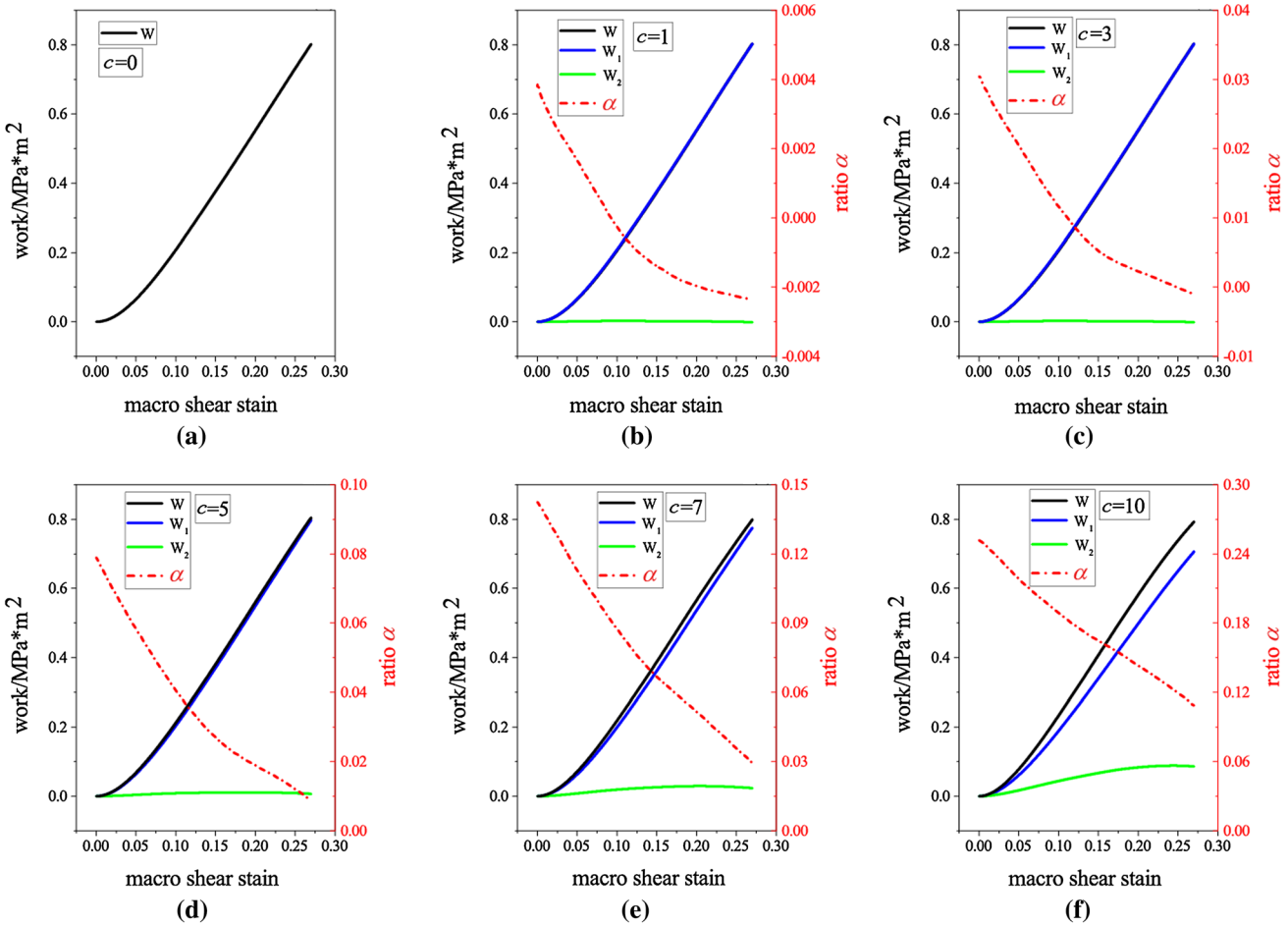

Fig. 6 Work and ratio α versus macro shear strain curves under six displacement patterns of ratio c, set as **a** 0; **b** 1; **c** 3; **d** 5; **e** 7; **f** 10, assembly with same radius of 0.001 m and porosity of 0.11

order work is the integral of macro shear stress times the macro shear strain in total volume, where the third order work is the integral of third order stress times the first shear strain gradient in total volume.

For all assemblies, the same phenomenon is observed, as presented in Fig. 6. Under low strains, when the same macro shear strain is achieved, as the first shear strain gradient increases, the second order work W_1 has not change, the third order work W_2 increases, while the ratio α increases. Under high strains, when the same macro strain is achieved, as the first shear strain gradient increases, the second order work decreases, the third order work increases and the ratio α also increases. By contrast, the tendency of the total work differs from various assemblies.

As described in Sect. 4.1, the effects of first shear strain gradient on the macro shear stress and the conjugated stress are different, which cause the different tendencies of the second order work, the third order work and the total work. As presented in Fig. 6, for one assembly in the same displacement pattern, the ratio α displays a downtrend. When the gradient is low, the ratio α is low under all deformation processes, which can be ignored. Adversely, when the gradient becomes higher, the ratio α becomes higher which cannot be ignored. The reason is that in the calculation equation of the macro stress and the conjugated stress, the macro stress is related to l_j^c, and the conjugated stress is related to J_j^c, which lead to the tendency decrease of ratio α under the entire deformation process.

When the same macro shear strain is achieved, as the first shear strain gradient increases, all quantities including the second work, the third work, the total work and the ratio α highly change. Figure 7 shows the tendencies of different assemblies when the ratio c is set to 10. Although the ratio α presents a downtrend in the entire deformation

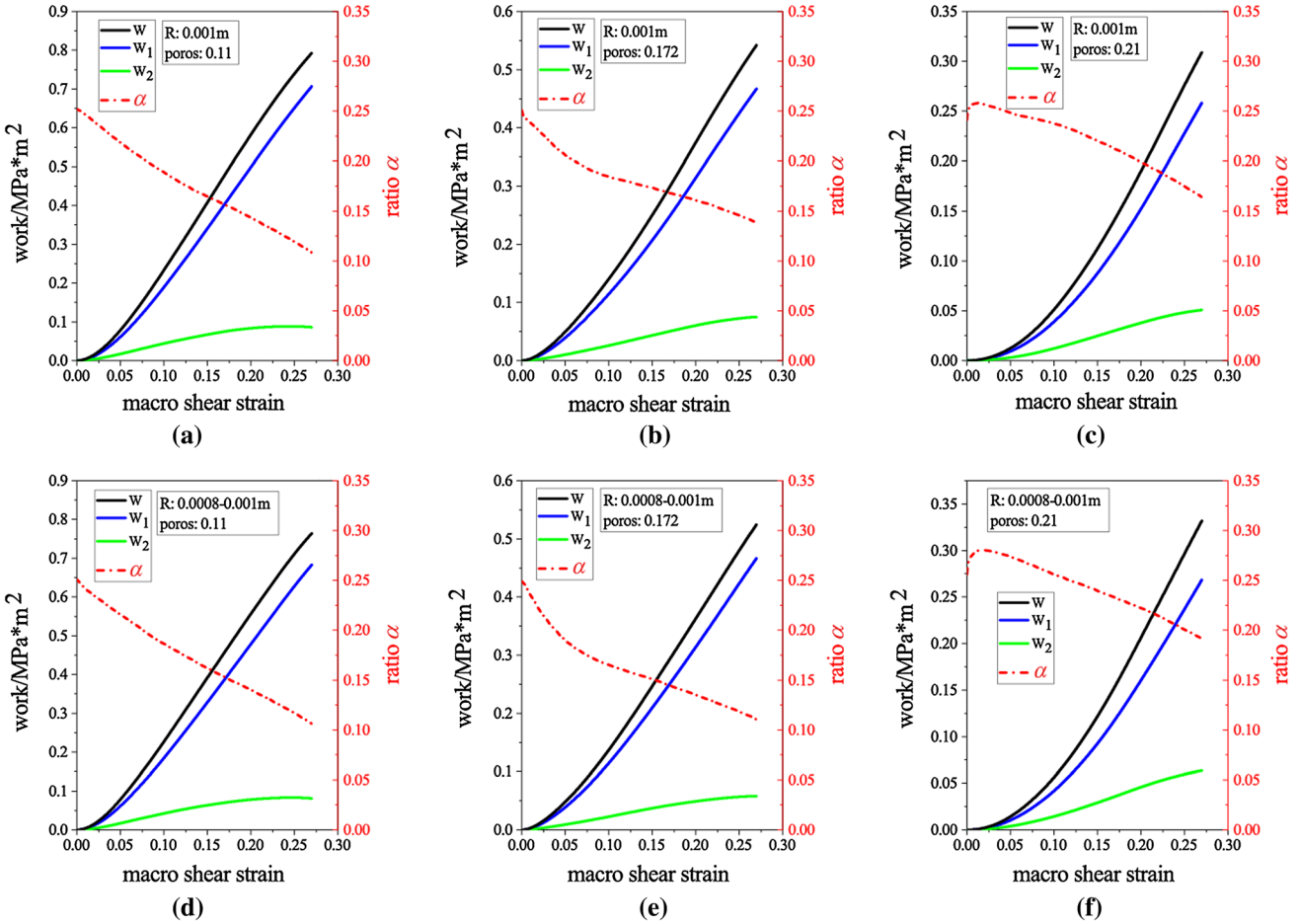

Fig. 7 Work and ratio α versus macro shear strain curves under same displacement patterns of ratio c, set as 10 for assembly of: **a**–**c** same radius 0.001 m; **d**–**f** 0.0008–0.001 m; and porosity of **a**, **d** 0.11; **b**, **e** 0.172; **c**, **f** 0.21

process, the effect on the work cannot be ignored, when the final strain is achieved, as the porosity increases, the ratio α for the assembly of 0.001 m increases from 10.9 to 16.4%, the ratio α for the assembly of 0.0008–0.001 m increases from 10.6 to 19.1%, where the change of ratio α is different from the macro shear stress.

4.3 Evolution of third order stresses invariants

In Sect. 4.1, the evolution of the third order stress $\overline{\Sigma}_{221}$ is described, which is conjugated to the second derivation of the displacement U_1 to the x_2 orientation, not revealing the local relative vertical displacement under different displacement patterns. Consequently, the other third order stresses should be considered, while the invariants $(F_1, F_2, F_3, F_4, F_5)$ of third order stresses are introduced to describe the evolution of the local vertical relative vertical displacement. The invariants of third order stresses are quadratic invariants, because $\overline{\Sigma}_{ijk}$ is equal to $\overline{\Sigma}_{jik}$, the third order stresses have six independent stresses, which form five invariants.

Figure 8 presents the changes of five invariants, for which, the change tendencies are the same under different displacement patterns, which fluctuate upwards and downwards, but as the first shear strain gradient increases, the amplitude of invariants variation increases. Also, the fluctuation is increasingly abrupt. Through analysis, the fluctuation has a close relationship with the third order stresses, including all $\overline{\Sigma}_{112}$, $\overline{\Sigma}_{122}$ and $\overline{\Sigma}_{222}$, for which, the changes also fluctuate. This is interpreted that the local relative vertical displacement tremendous change of an assembly produces the localization of particles.

Under a displacement pattern with gradient, the localization is quite apparent in all granular assemblies. As presented in Fig. 9, the vertical displacement change is big, which leads to the upward and downward movement of particles and produces the localization phenomenon. Since the displacement pattern controls the horizontal displacement and sets free the vertical displacement, the type of

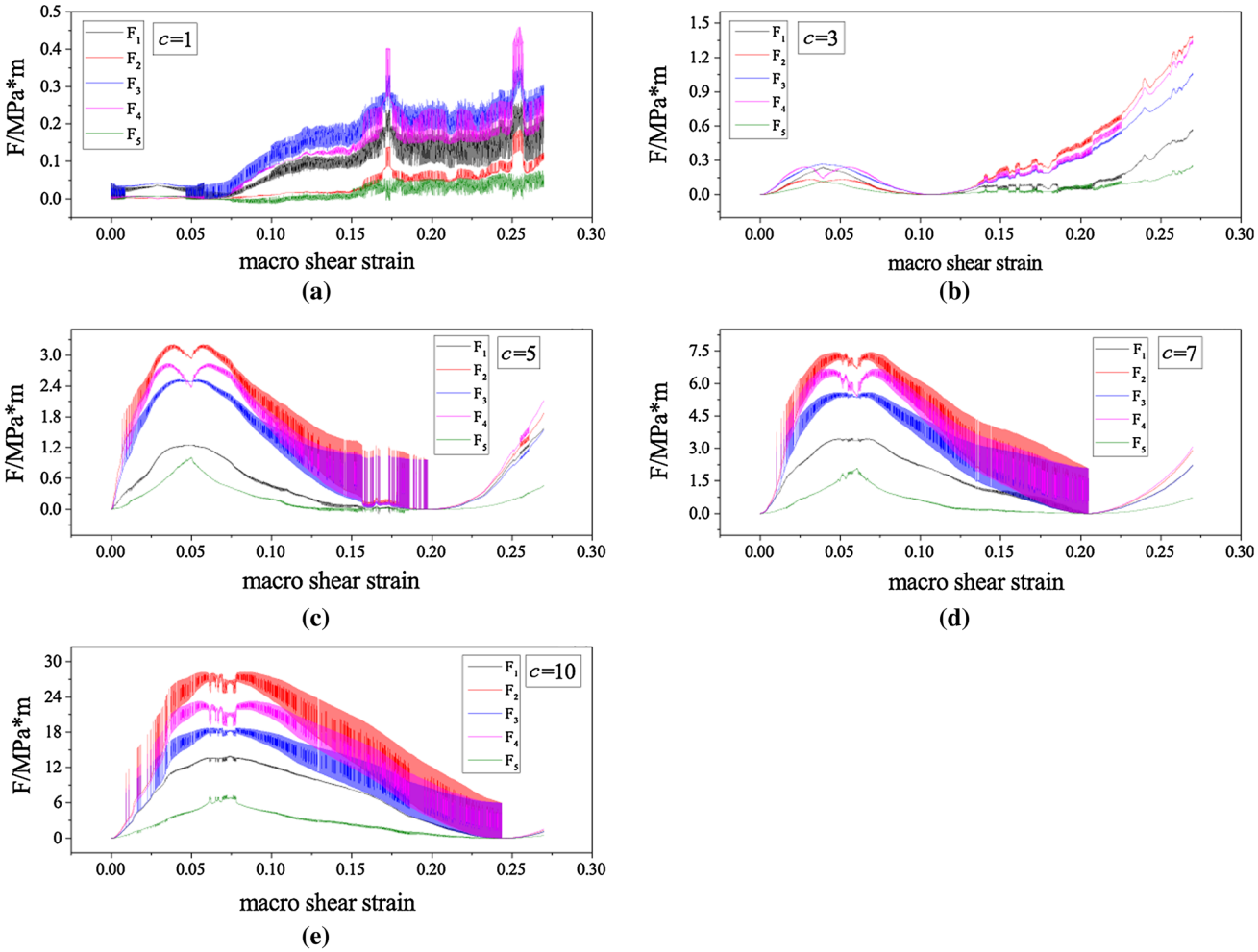

Fig. 8 Invariants versus macro shear strain curves under five displacement patterns of ratio c, set as **a** 1; **b** 3; **c** 5; **d** 7; **e** 10, assembly with same radius of 0.001 m and porosity of 0.11

localization is shear deformation. For an assembly, the first shear strain gradient is higher, the centralization of localization is easier, which cause the changes of the third order stresses under different displacement patterns. When the porosity or the particle radius of an assembly changes, the same phenomenon can be observed, but the macro shear strain of the localization initiation differs.

5 Conclusions

DEM simulations are carried out to investigate the effects of first shear strain gradient on the mechanical behaviors of different granular assemblies with various porosities and various particle radii. The important conclusions are summarized as follows.

(1) For all assemblies, when the first shear strain gradient increases, the conjugated stress $\overline{\Sigma}_{221}$ increases, the macro shear stress $\overline{\sigma}_{12}$ has no apparent change under low strains, but it changes apparently under high strains. When the first shear strain gradient exceeds one certain value, the gradient has a softening effect on the macro shear stress $\overline{\sigma}_{12}$. Moreover, for assemblies with different porosities or particle radii, the same change tendencies can be observed, but the extent of the effects will differ.

(2) For all assemblies, the change tendency of ratio α versus macro shear strain has a downtrend in the entire deformation process, but when the same macro shear strain is reached, as the first shear strain gradient increases, the values of the third order work W_2 and the ratio α increase. This is interpreted as the effects of the first shear strain gradient on the third order work could not be ignored. For assemblies with different porosity values or particle radii, the extent of the effects will differ.

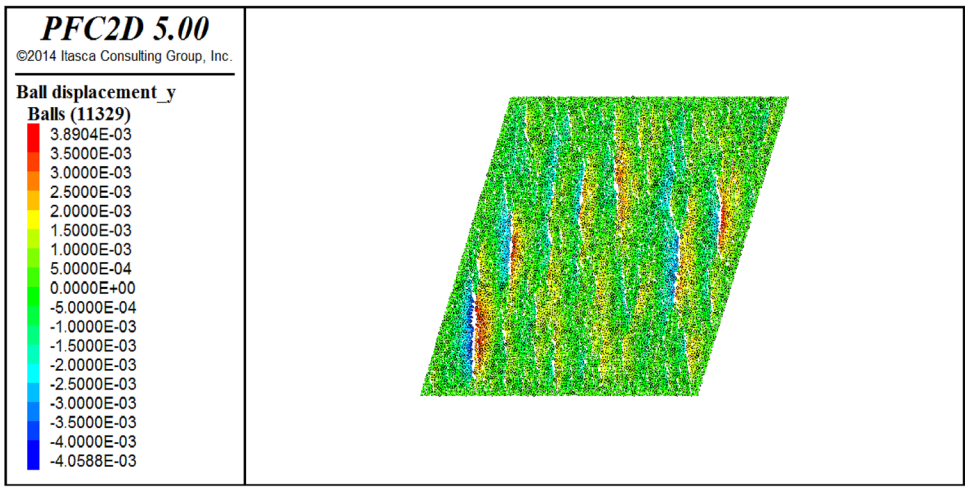

(a)

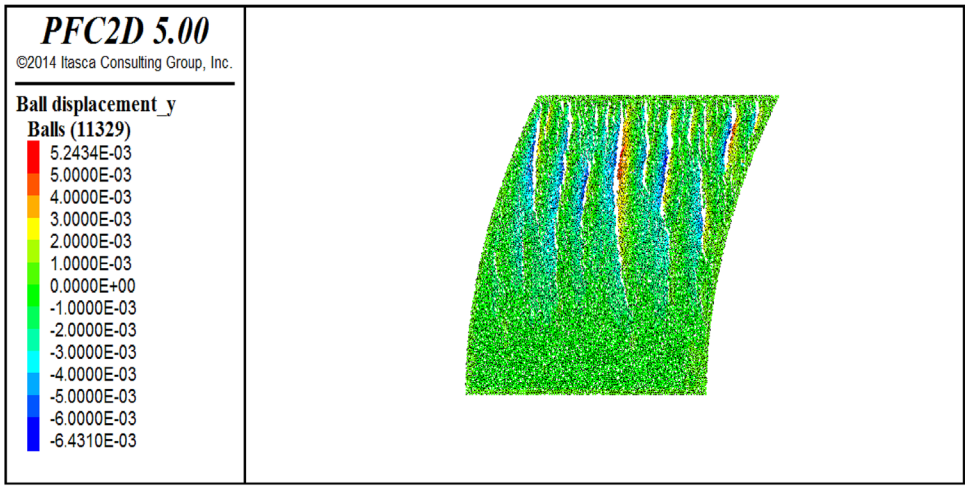

(b)

Fig. 9 Vertical displacement diagram under two displacement patterns of ratio c, set as **a** 0; **b** 10, assembly with the same radius of 0.001 m and porosity of 0.11

(3) For all assemblies, the invariants of the third order stresses explain the local relative vertical movement of particles. When the first shear strain gradient increase, the change amplitudes of F_1, F_2, F_3, F_4 and F_5 increase, which reveals that the local relative vertical displacement of particles are very acute and generates centralized localization. When the assembly has different porosities or particle radii, the extent of the effects will differ.

In summary, when the same macro shear strain is reached, the effects of the first shear strain gradient effect on the macro shear stress are not apparent under low strains, by contrast, as the first shear strain gradient increases, the third order stress $\overline{\Sigma}_{221}$, the third order work W_2 and the ratio α increase. From the view of work analysis for the mechanical behaviors in granular materials, it is necessary to consider the first shear strain gradient effects through the third order work classification into strain energy (not sliding energy). Therefore, the third order work as a part of strain energy and effects of the first shear strain gradient on the mechanical behaviors of granular materials cannot be ignored.

Acknowledgements The work was supported by National Natural Science Foundation of China (NSFC) (Grant Nos. 11711530643 and 11772236).

Compliance with ethical standards

Conflict of interest The authors declare that they have no conflict of interest.

References

1. Cambou, B.: Behaviour of Granular Materials. Springer, Wien (1998)

2. Hill, J.M., Selvadurai, A.P.S.: Mathematics and Mechanics of Granular Materials, pp. 1–9. Springer, Dordrecht (2005)
3. Hashin, Z.: Analysis of composite materials—a survey. J. Appl. Mech. **50**(3), 481–505 (1983)
4. Strack, O.D.L., Cundall, P.A.: The Distinct Element Method as a Tool for Research in Granular Media. University of Minnesota, Minneapolis (1978)
5. Noll, W.: A Mathematical Theory of the Mechanical Behavior of Continuous Media. Springer, Berlin (1974)
6. Noll, W.: A new mathematical theory of simple materials. Arch. Ration. Mech. Anal. **48**(1), 1–50 (1972)
7. Kuhn, M.R.: An experimental method for determining the effects of strain gradients in a granular material. Commun. Numer. Methods Eng. **19**(8), 573–580 (2003)
8. Kuhn, M.R.: Are granular materials simple? An experimental study of strain gradient effects and localization. Mech. Mater. **37**(5), 607–627 (2005)
9. Mindlin, R.D.: Second gradient of strain and surface-tension in linear elasticity. Int. J. Solids Struct. **1**(4), 417–438 (1965)
10. Fleck, N.A., Muller, G.M., Ashby, M.F., Hutchinson, J.W.: Strain gradient plasticity: theory and experiment. Acta Metall. Mater. **42**(2), 475–487 (1994)
11. Fleck, N.A., Hutchinson, J.W.: Strain gradient plasticity. Adv. Appl. Mech. **33**, 295–361 (1997)
12. Yang, F., Chong, A.C.M., Lam, D.C.C., Tong, P.: Couple stress based strain gradient theory for elasticity. Int. J. Solids Struct. **39**(10), 2731–2743 (2002)
13. Gao, H., Huang, Y., Nix, W.D., Hutchinson, J.W.: Mechanism-based strain gradient plasticity—I. Theory. J. Mech. Phys. Solids **47**(6), 1239–1263 (1999)
14. Yang, Y., Misra, A.: Micromechanics based second gradient continuum theory for shear band modeling in cohesive granular materials following damage elasticity. Int. J. Solids Struct. **49**(18), 2500–2514 (2012)
15. Placidi, L., Andreaus, U., Corte, A.D., Lekszycki, T.: Gedanken experiments for the determination of two-dimensional linear second gradient elasticity coefficients. Zeitschrift Für Angewandte Mathematik Und Physik **66**(6), 3699–3725 (2015)
16. Chang, C.S., Gao, J.: Second-gradient constitutive theory for granular material with random packing structure. Int. J. Solids Struct. **32**(16), 2279–2293 (1995)
17. Chang, C.S., Kuhn, M.R.: On virtual work and stress in granular media. Int. J. Solids Struct. **42**(13), 3773–3793 (2005)
18. Vardoulakis, I.: Strain Localization in Granular Materials, pp. 339–400. Springer, Vienna (1998)
19. Voyiadjis, G.Z., Alsaleh, M.I., Alshibli, K.A.: Evolving internal length scales in plastic strain localization for granular materials. Int. J. Plast. **21**(10), 2000–2024 (2005)
20. Hattamleh, O.A., Muhunthan, B., Zbib, H.M.: Gradient plasticity modelling of strain localization in granular materials. Int. J. Numer. Anal. Meth. Geomech. **28**(6), 465–481 (2004)
21. Rathbun, A.P., Marone, C.: Effect of strain localization on frictional behavior of sheared granular materials. J. Geophys. Res. Atmos. **115**(B1), 414–431 (2010)
22. Misra, A., Poorsolhjouy, P.: Granular micromechanics model of anisotropic elasticity derived from Gibbs potential. Acta Mech. **227**(5), 1–21 (2016)
23. Misra, A., Poorsolhjouy, P.: Granular micromechanics based micromorphic model predicts frequency band gaps. Continuum Mech. Thermodyn. **28**(1–2), 215–234 (2016)
24. Chang, C.S., Liao, C.L.: Constitutive relation for a particulate medium with the effect of particle rotation. Int. J. Solids Struct. **26**(4), 437–453 (1990)
25. Chang, C.S., Gao, J.: Kinematic and static hypotheses for constitutive modelling of granulates considering particle rotation. Acta Mech. **115**(1), 213–229 (1996)
26. Bardet, J.P., Vardoulakis, I.: The asymmetry of stress in granular media. Int. J. Solids Struct. **38**(2), 353–367 (2001)
27. Bagi, K.: Microstructural stress tensor of granular assemblies with volume forces. J. Appl. Mech. **66**(4), 934–936 (1999)
28. Bonelli, S., Millet, O., Nicot, F., Rahmoun, J., Saxcé, G.D.: On the definition of an average strain tensor for two-dimensional granular material assemblies. Int. J. Solids Struct. **49**(s 7–8), 947–958 (2012)
29. Spencer, A.J.M.: Part III-Theory of invariants. Mathematics **1**, 239–353 (1971)
30. Smith, G.F., Younis, B.A.: Isotropic tensor-valued polynomial function of second and third-order tensors. Int. J. Eng. Sci. **43**(5–6), 447–456 (2005)
31. Finite Element Method Set: Invariants of Second-Order Tensors—The Finite Element Method Set, Appendix B, 6th edn, pp. 604–608 (2005)
32. Rashid, M.A., Ahmad, F., Amir, N.: Linear invariants of a cartesian tensor under SO (2), SO (3) and SO (4). Int. J. Theor. Phys. **50**(2), 479–487 (2011)
33. Cundall, P.A.: Computer simulations of dense sphere assemblies. Stud. Appl. Mech. **20**, 113–123 (1988)
34. Cundall, P.A., Strack, O.D.L.: A discrete numerical mode for granular assemblies. Géotechnique **29**(1), 47–65 (1979)
35. Cundall, P.A., Strack, O.D.L.: Modeling of microscopic mechanisms in granular material. Stud. Appl. Mech. **7**, 137–149 (1983)